JOURNAL OF CATALYSIS 106, 202–209 (1987)

Analysis of the Morphology of High Surface Area Solids: Studies of Agglomeration and the Determination of Shape

WILLIAM CURTIS CONNER, JR.,*,[1] C. BLANCO,† K. COYNE,*
J. NEIL,* AND J. PAJARES†

*Department of Chemical Engineering, University of Massachusetts, Amherst, Massachusetts 01003, and †Instituto Catalisis y Petroleoquimica, Madrid, Spain

Received September 3, 1986; revised February 17, 1987

Characterization of the morphology of high surface area solids is most often accomplished by nitrogen desorption and/or mercury intrusion porosimetry. If the void/solid structure is viewed as an interconnected network, ad-de-sorption and retraction/intrusion may be associated with the openings and constrictions within the void network. This more realistic view adds another dimension to the analyses. The data can be analyzed as if the data consisted of agglomerated microspheres. This analysis proves consistent for compacted aerosol silicas but is inconsistent if the solid has a different morphology. More significantly, the ratios of the measured most probable radii of intrusion to those of retraction seem to be characteristic of the void solid structure and pore shapes, and thereby, it may be possible to infer the pore shapes and general structure from this more detailed analysis. A heuristic diagram of these trends is presented.

INTRODUCTION

Mercury porosimetry has been used as a method of determining pore-size distributions since the work of Ritter and Drake (*1*). Analysis of mercury intrusion and retraction data are based on the Washburn equation, viz.:

$$Pr = -2\gamma \cos \phi$$

where P is the pressure, r the radius, γ the surface tension of mercury, and ϕ the contact angle between the mercury and solid surfaces. An assumption in this analysis is that the pores are nonintersecting.

Porosimetry is an indirect analytical technique in that there is no direct method of determining the sample morphology from the pressure–volume relationship. The manner in which porosimetry data is interpreted depends upon the pore-structure model used. Lowell and Shields (*2*) interpret the data assuming that all pores are nonintesecting and attribute the hysteresis between the intrusion and retraction curves to a change in contact angle θ. This model does not reflect the known complexity of void structure for high surface area materials. Therefore, information gained from this analysis is of limited use.

Conner and Lane (*3*) have viewed porosimetry as a network process. The network model was originally envisioned to consists of spherical pores connected by volumeless, cylindrical throats. For this system, it was found that the throats controlled the intrusion process and the pores controlled the retraction process. This difference in controlling dimensions explains the hysteresis. The sequential nature of intrusion and retraction affects the measured throat-size and pore-size distributions (TSD and PSD). On intrusion, at a given pressure, some of the "open" throats ($r > 2\gamma \cos \theta/P$) are not penetrable (due to their inaccessibility to the mercury meniscus) and some of the "penetrable" throats (accessible to a mercury meniscus) are not open (because their radius is less than $-2\gamma \cos \theta/P$). As the pressure is increased, smaller throats become "open" and allow access to the large throats. The result is that the measured

[1] To whom correspondence should be addressed.

0021-9517/87 $3.00

TSD is shifted toward smaller radii (away from the actual distribution).

Similar effects are noted during retraction. For mercury to retract from a pore, (i) a continuous mercury path must exist to the exterior, and (ii) an interface (meniscus) must exist in one of the throats. In the initial stages of extrusion, involving smaller pores, fewer pores are open (because fewer menisci are available), and hence the number of pores with a given radius is underestimated. For larger pores, the last to retract have a greater probability of being stranded. Thus, the number of small pores is underestimated, the number of medium pores is overestimated, and the number of large pores is underestimated (*4*).

Another means of determining pore-size distributions is nitrogen sorption (adsorption and desorption). It has been shown that porosimetry and sorption give similar results for aerosil agglomerates (*5*); when comparing porosimetry and sorption, intrusion corresponds to desorption and extrusion corresponds to adsorption. The surface area can be estimated from sorption data using the method of Brunauer, Emmett, and Teller (BET) (*6*). Surface area can also be determined from porosimetry data, but BET surface area is by far the reliable measure, due to the differences in the assumptions made for each technique.

This three-dimensional network perspective for high surface area solids was first introduced in 1983 and has not been universally accepted. Few studies include both intrusion and extrusion or both adsorption and desorption data for samples. It is therefore necessary to further evaluate this perspective with a more detailed analysis. If this view proves to be consistent, the knowledge about the dimensions of the constrictions (throats) and openings (pores) within the void network in conjunction with the independently measured surface area gives added dimension to our analysis of void morphology.

The porosimetry data and BET surface area may be used in concert to deduce void/solid morphology. To see how the data could be used, it was necessary to use a well-characterized void–solid system for study. Compacted, monodispersed particles of varying shapes were used as model systems in this study. The initial focus was on compacted microspheres with void fractions around 50%; these systems can reasonably be approximated as a cubic lattice. Also, compacted nonspherical particles (rodlike, needlelike, and platelike structures), controlled pore glasses and other high surface area samples were studied for comparison. The goal was to find experimental differences among the samples which might be characteristic of the void/solid morphologies.

Each of these techniques (i.e., porosimetry, sorption, void fraction, and BET surface area) have been used independently to characterize the void and solid structure. In concert with the void structure viewed as a three-dimensional network a more detailed analysis was attempted. The initial approach is to subdivide morphologies into networks with low, medium, or high connectivities, into void structures created by platelets, needles, rods, or cracks and fissures, or into a solid riddled with holes. Data obtained for the model systems in this study are analyzed to deduce these basic morphological types.

Indeed we found that samples with differing pore shapes (created by the agglomeration of different-shaped particles) have fundamental differences in their data. Whereas compacted monodispersed particles were the primary focus of these studies, the analysis and conclusions are not limited to interparticle void morphologies. As an example, samples whose void space is made up of cracks and fissures will respond to these analytical techniques in the same manner as a sample made from compacted platelike particles.

EXPERIMENTAL

The porosimetry studies were conducted with a Quantachrome "Autoscan" poros-

imeter. Prior to intrusion the samples were evacuated to less than 200 Torr. The most probable radii of intrusion and extrusion were taken from the maxima of the derivative curves of the experimental plots, (dV/dP) vs P; the maxima pressures were converted to radii via the Washburn equation using $\gamma = 475$ dynes/cm and $\theta = 140$. The surface area was measured using a conventional BET apparatus. The "conventional" static system was assembled from parts originally fabricated and used in Professor Emmett's laboratory at The Johns Hopkins University. They were inherited in 1979.

Data were gathered on samples of agglomerated microparticles of uniform size and shape measured be electron microscopy. The agglomerates were formed by compacting the particles at pressures up to 60,000 psi in a 1-in.^{2} cylindrical die. Degussa aerosils were used for the compacted spherical particles; compacted MoO_2, MoO_2, and Kaoline for plateletlike structures; compacted Attapulgites and Bentonites for needlelike structures; iron hydroxides (β-FeOOH) for the monodispersed rodlike particles. Data were also gathered on controlled pore glasses (CPGs) from Electro-Nucleonics; aluminas provided by Gulf; and silica samples from Philadelphia Quartz and Shell Chemical Corp.

ANALYSIS

The basis of the analysis is first to interpret the data based on a model system consisting of compacted microspheres. Based on this view, we will analyze the pore-throat size distributions in terms of characteristic solid and void dimensions (i.e., r_s, a characteristic solid radius, and r_v, a characteristic void radius). These approaches utilize the measured void fractions and BET surface areas in combination with the distributions of pore and throat sizes measured by porosimetry (or the corresponding sorption studies). These data are taken in various combinations to calculate the characteristic dimensions. The samples are analyzed on these bases to determine if a consistent picture is found for the spherical agglomerates and where deviations are found for the agglomerated nonspherical particle systems. We will use this to deduce how this morphological data may be used to infer the nature of the void and solid structures and the corresponding void shapes.

First consider the model system represented by a simple cubic packing (scp) of spheres; the scp unit cell is depicted in Fig. 1. The solid portion of the cell is shown on the left and the void portion is illustrated on the right. The openings on the six faces of the unit cell correspond with the throat of the network and the void space within the cell corresponds with the pore(s). The connectivity (the number of interconnections between pores) for this geometry is six.

The void fraction v_f of a scp is 0.48. The intrusion radius r_i and the retraction radius r_r can be first estimated from an "inscribed circle (throat) or sphere (pore)" method: r_i is the largest circle that can be inscribed between the spheres on the face of the unit cell, and r_r is the radius of the largest sphere that can be inscribed inside the cell. This method disregards the effective hydraulic radii, assuming the ratios are the same. For a scp the ratio r_r/r_i would be 2.4. This is illustrated in Fig. 2 where the eight spheres that are part of the unit cell are depicted on the left rotated by 45° around the vertical axis as is a plane through the center of the cell parallel to this axis. The circles of intersection of the four diagonally oppposing spheres with this plane are illustrated on the right. The inscribed sphere corresponding to r_r (now a circle in the plane) and r_i are also represented.

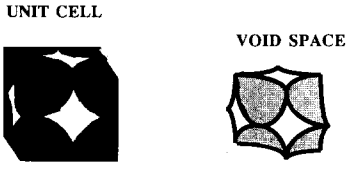

FIG. 1. Unit cell of a simple cubic packing, scp, of spheres shown at the left. The void structure within the unit cell is depicted on the right.

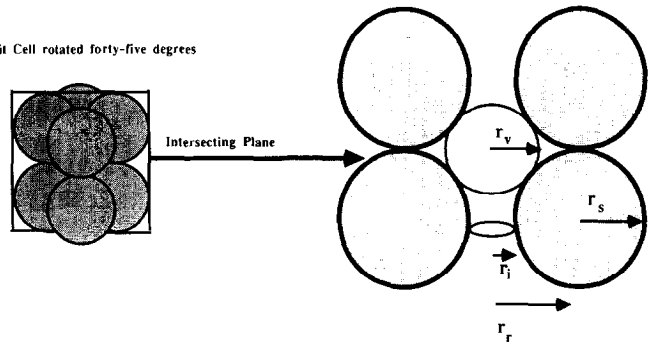

FIG. 2. Schematic cross section of a unit cell showing the diagonal spheres and the "effective" values for the measured radii of intrusion r_i and retraction r_r, and the calculated characteristic radii of the solid r_s and void r_v (see text for details).

Additional physical parameters can be derived based on this assumed morphology. A characteristic equivalent radius of the spheres (solid structural units) can be estimated from the ratio of the solid volume V to the surface area SA; for spheres, this ratio equals $r/3$, where r is the solid radius. Thus the radius of the sphere could be estimated as

$$r_s = 3(V/SA) \quad (1)$$

where the subscript "s" denotes the solid.

The solid radius can also be estimated, as illustrated in Fig. 2, as the difference between the measured radii of retraction and intrusion, viz.,

$$r_s = r_r - r_i \quad (2)$$

A similar analysis of the void structure can be done. Because the void structure is irregularly shaped, a spherical void geometry is assumed to calculate an effective void radius r_v. Using a similar approach as in Eq. (1) for r_s, we obtain

$$r_v = 3(V_i/SA) \quad (3)$$

where V_i is the volume of mercury intruded. Note that the surface area of the solid and the surface area of the void would be identical if we assume that the mercury totally wets the solid surface at the highest pressure employed (to 60,000 psig in our apparatus).

In a scp, there is one pore for each sphere. N, the number of pores (or spheres), can be calculated if r and SA are known. We can use Eq. (2) and $N = SA/4\pi r_s^2$. Since the volume of a single pore equals V_i/N,

$$r_v = [(3V_i(r_r - r_i)^2)/SA]^{1/3} \quad (4)$$

A third expression for r_v can be derived through another analysis of the unit cell, attributing void fraction changes to changes in the unit cell dimensions and using Eq. (2),

$$r_v = [(V_f(r_r - r_i)^3/(1 - V_f)]^{1/3} \quad (5)$$

All of the above parameters [i.e., V_f, r_r/r_i, and Eqs. (1)–(5)] use porosimetry data and the measured surface areas. Note that the different methods for estimating r_s and r_v are, for the most part, independent of each other. This allows us to compare the same parameters estimated from different methods. Thus we can (a) compare experimental and theoretical void fractions and (r_r/r_i) values, and (b) compare calculated r_s and r_v values among each other in this "spherical packing analysis."

RESULTS AND DISCUSSION

The raw data for the compacted microspheres, Aerosils, are shown in Table 1. The listed intrusion and retraction radii are from the maxima in the dV/dP vs pressure curves. The calculated solid and void radii r_s and r_v based on the various equations (1)–

TABLE 1

Morphological Characteristics (Porosimetry and Surface Area) of Compacted Microspheres

Microsphere	Intrusion radius (*A*)	Extrusion radius (*A*)	Surface area (m^2/g)	Hg intruded (cc/g)	Compaction pressure (psi)
Aerosil 130	119	255	106	0.773	30,000
Aerosil 200	93	188	165	0.807	30,000
Aerosil 300	59	119	300	0.920	30,000
Aerosil 380	32	72	360	0.483	30,000
Aerosil OX-50	176	487	43	0.487	20,000
Aerosil MOX-80	108	281	66	0.502	30,000
Aerosil H-55	50	107	220	0.746	30,000
Aerosil R805	56	143	150	0.944	30,000
Aerosil R812	35	77	230	0.919	30,000
Aerosil R972	82	173	170	0.903	20,000
Aerosil R974	64	143	164	1.248	30,000

(5) are shown in Table 2. The corresponding values for the solid and void radii agree within an average of 10%; although a few (e.g., r_s for R812) differ by up to 20%. This suggests that even though the corresponding calculations are based on different combinations of data sources the perspective of a void network comprising interconnected constrictions, *throats,* and openings, *pores,* is consistent. Further, the estimated relationships found for a scp of spheres pertains to the combined techniques in the analyses. We anticipate that nonspherical agglomerates will not yield this consistency in calculated solid and void radii.

As the samples of agglomerated particles are compressed, the void fraction decreases. As an example, the effect of compression on the smallest microspheres (Aerosil 380 with 7-nm particles) is shown in Table 3. The calculated values for the characteristic void dimension r_v decreases with the void fraction decrease for each method by which it is calculated, as expected. For the calculation of the characteristic solid dimension r_s the estimate based on surface to volume ratio calculations does not change [Eq. (1)], whereas the estimate based on the porosimetry data viewed as a scp of spheres does change. As the void fraction decreases the scp approximation is increasingly accurate and the values for r_s converge. Surprisingly, the ratios of the measured radii of extrusion to intrusion did not vary from sample to sample (Table 1) or for samples as a function compression and the concomitant decrease in

TABLE 2

Spherical-Packing Analysis of Compacted Microspheres (Sizes in Å)

Microsphere	Void fraction	r_e/r_i	r_s		r_v		
			(1)	(2)	(3)	(4)	(5)
Aerosil 130	0.57	2.14	129	136	172	147	150
Aerosil 200	0.56	2.02	83	95	106	98	103
Aerosil 300	0.56	2.02	45	60	59	60	65
Aerosil 380	0.45	2.25	38	40	31	37	38
Aerosil OX-50	0.50	2.77	317	311	313	312	310
Aerosil MOX-80	0.51	2.60	207	173	213	185	175
Aerosil H-55	0.51	2.14	62	57	65	59	58
Aerosil R805	0.47	2.55	91	87	82	85	84
Aerosil R812	0.42	2.20	59	42	42	42	38
Aerosil R972	0.58	2.11	80	91	109	97	101
Aerosil R974	0.55	2.23	83	79	103	86	85

TABLE 3

Effect of Compression—Aerosil 380

Compaction pressure (psi)	Void fraction	r_e/r_i	r_s		r_v		
			(1)	(2)	(3)	(4)	(5)
1,000	0.59	2.1	38	64	55	61	73
10,000	0.54	2.3	38	57	45	53	60
20,000	0.46	2.1	38	44	32	40	42
30,000	0.45	2.3	38	40	31	37	38

void fraction (Table 2). The measured ratios were all within 2.38 ± 15%. For a scp of spheres, the void fraction would be 48% and the ratio would be 2.4. It seems that there is a geometric regularity created by the agglomeration of spheres whereby the relationship between the measured dimensions of the constrictions and openings is retained independent of the void fraction. As discussed below it seems to be a characteristic of solids that may be represented as compacted spheres.

Table 4 shows similar analysis for the compaction of nonspherical particles and other high surface area solids. Recall that β-FeOOH is rodlike, Kaoline and the Molybdenas are platelike, and the Attapulgite and Bentonite are needlelike. Equations (1) and (2) are used to calculate equivalent solid radii and the corresponding equations (3) and (5) are used to calculate the equivalent void radii for each sample. Note that Eqs. (1) and (3) are dependent on the surface areas and void volume independent of the pore-size distribution, whereas Eqs. (2) and (5) are based on the porosimetry independent of the surface areas. There is no noticeable agreement between the solid and void radii calculated based on the corresponding equations. Except for r_s for MoO_3(B) (which is probably fortuitous), the differences are all *much* greater than the 10% found for the compacted microspheres. Further, there is no consistent trend in the estimates between the different analyses. These results confirm that the consistency found for the scp analysis of the data for spheres is not fortuitous; indeed, an interconnected network of constrictions (measured by intrusion and desorption) and openings (from extrusion and adsorption) is an effective model for the processes.

TABLE 4

Spherical-Packing Analysis of Nonspherical Samples

Sample	Void fraction	r_r/r_i	r_s (Å)		r_v (Å)	
			(1)	(2)	(3)	(5)
Controlled pore glasses						
CPG-332	0.74	4.4	173	638	504	911
CPG-486	0.50	4.9	317	1159	316	1157
β-FeOOH						
(A)	0.61	4.1	694	3691	1088	4287
(B)	0.63	5.0	556	3060	940	3645
Gulf aluminas						
SN3-4F90	0.73	3.2	68	147	182	204
SN3-4F92	0.69	3.1	74	129	169	170
Philadelphia Quartz silicas						
PQ 7	0.58	2.3	78	47	10	53
PQ 9	0.56	2.3	69	43	89	47
Kaoline	0.76	2–2.8	969	86	3026	126
Molybdenas						
MoO_2 (A)	0.5	1.6–2.4	35	59	36	59
MoO_2 (B)	0.71	1.5–2.2	52	55	128	74
MoO_3	—	1.6–1.9	34	24	57	29
Attapulgite	0.92	1.9–3.6	118	241	10,732	1083
Na bentonite	0.93	1.9–2.9	435	32	6380	78

For other void networks, such as created by the compaction of plates, rods, or needles, the relationship between the dimensions of the openings and the constrictions would be expected to differ from the network created by compacted spheres. Spheres pack more uniformly due to their axial symmetry. The other shapes (particularly rods and needles) have axes of different dimensions that can create a larger divergence between the constrictions and openings. As examples, needles and rods can be packed with their long axes oriented at up to right angles to each other. In a random packing larger void spaces will be created compared to the constrictions created if the axes are aligned. For plates, there is a tendency for them to stack "surface to surface" as larger angles between the surfaces would not be favored during compaction. Between platelike surfaces the relationship between openings and constrictions would be minimal. The anticipated result is that, compared to spheres, rods and needles will give a large ratio of the measured dimensions of the openings to the constrictions and the plates will give a lower ratio. The relationships between the dimensions of the constrictions and openings for each of these examples would be

expected to depend on the void fraction of the network, i.e., as the void fraction decreases, the dimensions of the openings would be expected to decrease faster than the dimensions of the constrictions.

The ratio of the measured radii of extrusion to that of extrusion for spheres was found to be consistently around 2.4. As seen in Table 4, the corresponding ratios for the other samples are not consistent with the data for compacted spheres. The rods and needles (represented by β-FeOOH, Attapulgite, and Bentonite) gave high ratios, >2.7, of the radii of extrusion to intrusion. The platelike agglomerates (represented by Kaoline and Molybdenas) gave low ratios of the measured radii, i.e., <2.1. The controlled pore glasses give high ratios as represented by CPG-332 and CPG-486. These are often considered to involve straight cylindrical pores; although microscopy reveals a porous network. The hysterisis reflected in the ratios of the measured radii has been cited to support the contention that hysterisis occurs for all samples. Recently, Shell has introduced a class of silicas, "Shell Silica Spheres," that are claimed to involve nonintersecting cylindrical pores. The intrusion and retraction porosimetry for a representative sample (980 D-2.2) is shown in Fig. 3. The steep intrusion and retraction curves indicate narrow distributions of sizes, as found for the CPGs. The coincidence of the intrusion and extrusion curves suggest that the samples are, indeed, made up of uniform nonintersecting pores. Many of these Shell samples exhibited similar coincidence for the intrusion and retraction curves; although not all of the samples that we studied gave evidence for the extent of coincidence as seen for this particular sample. This data confirms that hysterisis is not a universal phenomenon and seems to be dictated by the network void structure.

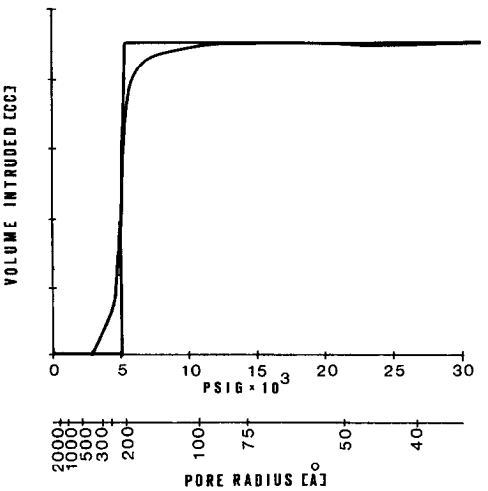

FIG. 3. Porosimetry of Shell Silica Spheres, 980 D-2.2, showing intrusion (lower curve) and retraction (upper curve).

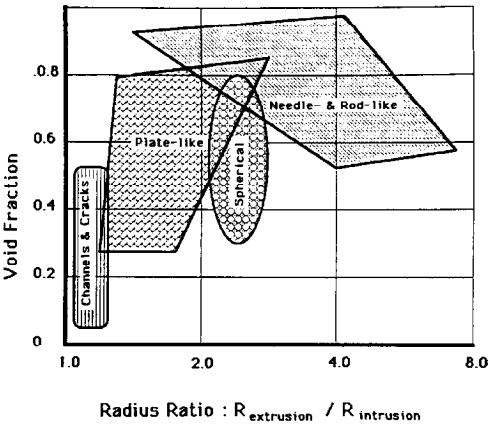

FIG. 4. Proposed heuristic diagram for the classification of void/solid morphologies as if the structures were formed by the agglomeration of homomorphic subparticles.

It seems that the easily calculated ratios of the radii of retraction (or adsorption) to those of intrusion (or desorption) are characteristic of the void morphology. As spheres, rods, needles, or plates yield different ratios, it may be possible to infer differing equivalent shapes from this calculation. Our data suggests a heuristic by which the equivalent structure, if viewed as an agglomerate of subparticles, may be inferred. This diagram is shown in Fig. 4. As noted above, this proposal is not limited to solids formed by the compaction of subparticles. Materials that behave as spherical (or

other) agglomerated morphological structures in porosimetry or sorption may not necessarily be spherical agglomerates but may exhibit similar transport/flow characteristics.

More importantly, this analysis suggests that changes in the ratio due to processing or pretreatment may be characteristic of a change in the porous network. Specifically, as the connectivity of the void network decreases (as would be expected from rods to spheres to plates) the ratio of the measured radii of retraction to intrusion decreases (>3, 3–2, <2). During processing, if the ratio decreases, this may be characteristic of solid reconstruction toward sheetlike structures, and if the ratio increases this may be characteristic of internal cracking to increase the interconnectivity.

ACKNOWLEDGMENTS

We wish to thank the U.S.–Spain Joint Committee for Scientific and Technical Cooperation, Grant 83-051, for the support of this research. We thank Gulf Oil Corporation, Philadelphia Quartz Corporation, and Professor Egon Matijević for generously providing samples. One of us, W.C.C., wishes to thank the NSF for the donation of the equipment and Chevron for their continued support.

REFERENCES

1. Drake, L. C., and Ritter, H. C., *Ind. Eng. Chem.* **17,** 787 (1945).
2. Lowell, S., and Shields, J. E., *J. Colloid Interface Sci.* **80,** 192 (1980); **90,** 203 (1982); *Powder Technol.* **29,** 37 (1980).
3. (a) Conner, W. C., Lane, A. M., Ng, K., and Goldblatt, M., *J. Catal.* **83,** 336 (1983); (b) Conner, W. C., Lane, A. M., and Hoffman, A., *J. Colloid Interface Sci.* **100,** 185 (1984); (c) Lane, A. M., Conner, W. C., and Ng, K., *Chem. Eng. Commun.*, in press.
4. (a) Lane, A. M., and Conner, W. C., *J. Catal.* **89,** 217 (1984); (b) Lane, A. M., Conner, W. C., and Shah, N., *J. Colloid Interface Sci.*, in press.
5. Conner, W. C., Cevallos-Candau, J. F., Weist, E. L., Pajares, J., Mendioroz, S., and Cortes, A., *Langmuir*, in press.
6. Brunauer, S., Emmett, P. H., and Teller, E., *J. Amer. Chem. Soc.* **60,** 309 (1938).